RESEARCH MEMORANDUM

A TRANSONIC WIND-TUNNEL INVESTIGATION OF THE AERODYNAMIC CHARACTERISTICS OF THREE 4-PERCENT-THICK WINGS OF SWEEPBACK ANGLES 10.8°, 35°, AND 47°, ASPECT RATIO 3.5, AND TAPER RATIO 0.2 IN COMBINATION WITH A BODY

By Ralph P. Bielat

Langley Aeronautical Laboratory
Langley Field, Va.

NATIONAL ADVISORY COMMITTEE
FOR AERONAUTICS

WASHINGTON

July 15, 1952

NATIONAL ADVISORY COMMITTEE FOR AERONAUTICS

RESEARCH MEMORANDUM

A TRANSONIC WIND-TUNNEL INVESTIGATION OF THE AERODYNAMIC CHARACTERISTICS OF THREE 4-PERCENT-THICK WINGS OF SWEEPBACK ANGLES 10.8°, 35°, AND 47°, ASPECT RATIO 3.5, AND TAPER RATIO 0.2 IN COMBINATION WITH A BODY

By Ralph P. Bielat

SUMMARY

An investigation was made in the Langley 8-foot transonic tunnel of the effect of sweepback angle on wing-body characteristics at Mach numbers varying from 0.50 to 1.12. Sweepback angles of 10.8°, 35°, and 47° based on the 0.25-chord line were investigated. Lift, drag, and pitching-moment coefficients were determined from strain-gage measurements. The Reynolds number of the tests based on the mean aerodynamic chord varied from 2.0×10^6 at a Mach number of 0.50 to 2.5×10^6 at a Mach number of 1.12.

An increase in sweepback angle from 10.8° to 47° had a small effect in increasing the lift-curve break Mach number. The drag-rise Mach number was delayed to higher values, the rate of drag increase after the drag-rise Mach number was reduced, and the Mach number where large losses in the values of maximum lift-drag ratio occurred was delayed as the angle of sweepback was increased. For the wings of the present investigation, the effect of sweep on the maximum pressure-drag coefficient could be calculated fairly accurately. An increase in sweepback angle reduced the rearward movement of the aerodynamic-center location as the Mach number increased from 0.50 to 1.10.

INTRODUCTION

The NACA has been conducting an investigation to determine the aerodynamic characteristics at supersonic speeds (references 1 to 3) and at transonic speeds of wings varying in thickness ratio and in sweep for use on a high-speed bomber. The effects of thickness ratio and of

thickened root sections on the aerodynamic characteristics at transonic speeds of wings with 47° sweepback, aspect ratio 3.5, and taper ratio 0.2 are reported in reference 4. The present paper presents the results of the aerodynamic characteristics of three 4-percent-thick wings of sweepback angles 10.8°, 35°, and 47° based on the 0.25-chord line, aspect ratio 3.5, and taper ratio 0.2 in combination with a body.

The results reported herein consisted of lift, drag, and pitching-moment measurements for a Mach number range of 0.50 to approximately 1.12. The tests were conducted in the Langley 8-foot transonic tunnel.

SYMBOLS

The aerodynamic coefficients and other symbols used in this paper are defined as follows:

A	aspect ratio of wing $\left(b^2/S\right)$
a	speed of sound in undisturbed stream, feet per second
b	span of wing, feet
C_D	drag coefficient (D/qS)
$\frac{dC_D}{dC_L{}^2}$	drag-due-to-lift parameter
C_{D_o}	drag coefficient at zero lift
C_D'	sonic pressure drag $\left(C_{D_{o(M=1.0)}} - C_{D_{o(M=0.6)}}\right)$
$C_D{}'_{max}$	maximum pressure drag $\left(C_{D_{o(max)}} - C_{D_{o(M=0.6)}}\right)$
C_L	lift coefficient (L/qS)
$C_{L_{(L/D)_{max}}}$	lift coefficient for maximum lift-drag ratio
C_{L_α}	lift-curve slope per degree $\left(dC_L/d\alpha\right)$
C_m	pitching-moment coefficient $\left(\frac{M_{\bar{c}/4}}{qS\bar{c}}\right)$

[redacted]

$\frac{dC_m}{dC_L}$	static-longitudinal-stability parameter
$\bar{c}$	wing mean aerodynamic chord, inches
D	drag, pounds
L	lift, pounds
$(L/D)_{max}$	maximum lift-drag ratio
M	Mach number (V/a)
$M_{\bar{c}/4}$	pitching moment of aerodynamic forces about lateral axis which passes through 25-percent point of mean aerodynamic chord of wing, inch-pounds
q	free-stream dynamic pressure, pounds per square foot $\left(\frac{1}{2}\rho V^2\right)$
R	Reynolds number based on $\bar{c}$
S	wing area, square feet
t/c	wing thickness ratio in percent of chord
V	free-stream velocity, feet per second
α	angle of attack of model, based on body reference axis, degrees
Λ	angle of sweep of wing, based on 25-percent-chord line, degrees
ρ	free-stream density, slugs per cubic foot

APPARATUS AND METHODS

Tunnel

The tests were conducted in the Langley 8-foot transonic tunnel which is a dodecagonal, slotted-throat, single-return type of wind tunnel. The use of longitudinal slots along the test section permitted the testing of the models through the speed of sound without the usual

[redacted]

choking effects found in the conventional closed-throat type of wind tunnel. Typical Mach number distributions along the center of the slotted test section in the region occupied by the model are shown in figure 1. Local deviations from the average free-stream Mach number were no larger than 0.003 at subsonic speeds. With increases in Mach number above 1.00, the deviations increased but did not exceed 0.010 at a Mach number of 1.13. A complete description of the Langley 8-foot transonic tunnel can be found in reference 5.

Model

The models employed for the tests were supplied by a U. S. Air Force contractor. The models represented midwing configurations and were constructed of steel. All the wing models were 4 percent thick in a streamwise direction, with aspect ratio of 3.5, taper ratio of 0.2, zero twist and dihedral, and the following airfoil section parallel to the model plane of symmetry:

Thickness distribution	NACA 65A series
Mean line ordinates	1/3 of NACA 230 series + NACA 6-series uniform-load mean line ($a = 1.0$) for $c_{l_i} = 0.1$

Sweep angle was the only geometric parameter which was varied on the models. Sweepback angles of 10.8°, 35°, and 47° based on the 0.25-chord line were investigated. The hollow steel bodies were built integrally with each of the wings and represented cylindrical bodies having ogive nose sections with a ratio of body diameter to wing span about 0.094. Photographs of the wing models are shown as figure 2, and dimensional details of the models are shown in figure 3. Airfoil coordinates are given in table I.

Model Support System

The models were attached to the sting support through a six-component, internal, electrical strain-gage balance which was provided by a U. S. Air Force contractor. Angle-of-attack changes of the models were accomplished by pivoting the sting about a point which was located approximately 66 inches downstream of the 0.25 mean aerodynamic chord. A 15° coupling located ahead of the pivot point was used in the sting in order to keep the model position reasonably close to the tunnel axis when the model angle of attack was varied from 6° to 12°. The angle mechanism was controlled from outside the test section and therefore permitted angle changes with the tunnel operating. A detailed description of the support system can be found in reference 6.

[redacted]

Measurements

Lift, drag, and pitching moment were determined by means of an electrical strain-gage balance located inside the body. In general, it was desired to make measurements for angles of attack from -2° to 12° at Mach numbers varying from 0.50 to approximately 1.12. Testing at high angles of attack at high subsonic and low supersonic Mach numbers, however, was limited by the pitching-moment design load of the balance. The accuracy of the data, based on the static calibration of the balance and the reproducibility of the data, is as follows:

C_L	± 0.01
C_D	± 0.001
C_m	± 0.004

A pendulum type of accelerometer calibrated against angle of attack located within the sting downstream of the models was used to indicate the angles of the models relative to the air stream under static conditions. For actual testing conditions, however, it was necessary to apply a correction to the angle of attack of the model because of the elasticity of the sting-support system.

The use of the calibrated accelerometer in conjunction with the remotely controlled angle-of-attack changing mechanism allowed the model angle to be set within $\pm 0.1^{\circ}$ for all test Mach numbers.

Reynolds Number

The variation of test Reynolds number, based on the mean aerodynamic chord of the wing, with Mach number averaged for several runs is presented in figure 4. The Reynolds number varied from 2.0×10^6 at a Mach number of 0.50 to 2.5×10^6 at a Mach number of 1.12.

CORRECTIONS

The usual corrections to the Mach number and dynamic pressure for the effects of model and wake blockage and to the drag coefficient for the effect of the pressure gradient caused by the wake are no longer necessary with the use of longitudinal slots in the test section (reference 7). The data presented herein have been corrected for a slight misalinement of the air stream in the tunnel.

The drag data have been corrected for base pressure such that the drag corresponds to conditions where the body base pressure is equal to the free-stream static pressure.

The bending of swept wings introduces a twist along the span which effectively changes the loading characteristics. The effects on the aerodynamic characteristics caused by bending of the swept wings were determined using the theoretical span loadings of reference 8 and the stiffness properties of the wings which were determined from static loads. The calculations were made for a Mach number of 0.70 and indicated that bending of the 35° and 47° sweptback wings did not materially change the aerodynamic characteristics of the data presented herein.

There exists a range of Mach numbers above Mach number 1.0 where the data are affected by reflected shock waves. On the basis of the results of reference 9, it was estimated that the reflected nose shock wave should clear the rear of the model at Mach numbers above 1.08. Schlieren pictures made during the present tests have substantiated these calculations. The results of reference 9 also indicate that although a detached bow wave exists on the model at low supersonic Mach numbers the reflected wave up to a Mach number of approximately 1.04 is of such weak intensity that the data are not appreciably affected. Accordingly, no data were taken in the range of Mach numbers from 1.04 to 1.08; and in the final crossplots of the results the curves are shown as dashed lines in this range of Mach numbers.

RESULTS AND DISCUSSION

An index of the figures presenting the results is as follows:

[redacted]

The reference axes of the data presented in the figures have been changed from body axes to wind axes. In order to facilitate presentation of the data, staggered scales have been used in many of the figures and care should be taken in identifying the zero axis for each curve. References to wings in this discussion refer to data presented for wing-body configurations unless otherwise noted. Data for the body-alone configuration can be found in reference 4.

Lift Characteristics

An increase in the angle of sweep from 10.8° to 47° had only a negligible effect on the lift-curve break Mach number at a lift coefficient of zero (fig. 8). The results indicated that the maximum increases in the lift-curve-slope values at zero lift coefficient for the wings of 10.8°, 35°, and 47° sweepback increased 69 percent, 53 percent, and 69 percent, respectively, above the values at a Mach number of 0.50. The large increase in the lift-curve slope for the wing of 47° sweepback was probably associated with the nonlinearities in the lift characteristics near zero lift at Mach numbers in the range from 0.94 to 1.00 (fig. 7(a)). It should be noted, however, that these nonlinearities depend upon the fairing as determined from the measured lift at a single angle of attack of -2° (see fig. 7(a)) and as a result the slope is subject to the well-known accuracy difficulties in the determination of lift-curve slopes. In any case, little significance is considered to be associated with these differences. The decrease in the values of the lift-curve slope above the lift-curve break Mach number was much less for the 10.8° sweptback wing than for the 35° and 47° sweptback wings.

Theoretical lift-curve slopes at zero lift are also included in figure 8. For the subsonic Mach number range, the lift-curve slopes at a Mach number of 0.50 were modified for the first-order effects of compressibility by an adaptation of the Prandtl-Glauert relation as given in reference 10. The theoretical lift-curve slopes at supersonic Mach numbers were calculated using the methods given in references 11 and 12. The agreement between the experimental results and theoretical results at subsonic Mach numbers for the 10.8° sweptback wing is good; however, the theoretical curves are seen to underestimate the compressibility effects at high subsonic speeds for the 35° and 47° sweptback wings which indicates the apparent inadequacies of the theory. The statement should be made, however, that the agreement between the experimental and theoretical lift-curve slopes for the 10.8° sweptback wing may be fortuitous inasmuch as the lifting-line theory of reference 10 was used. If the more rigorous methods were used to predict the effects of compressibility on the lift-curve slopes, such as the Weissinger modified lifting line (reference 8) or the Falkner lifting-surface methods, lower rates of increase in lift-curve slope with Mach number would be indicated and, therefore, would be in poor agreement with the experimental results. In the supersonic speed range the theoretical lift-curve slopes are

considerably higher than the experimental slopes. This difference is probably the result of wing thickness since the wings of the present investigation were of finite thickness; whereas the theory is for wings of zero thickness.

At a lift coefficient of 0.3, the lift-curve slopes for the three wings exhibited similar trends as at a lift coefficient of zero except that the maximum increases in C_{L_α} at high subsonic Mach numbers were generally less and decreased with increase in sweepback angle as would be predicted by theory.

Drag Characteristics

The effects of sweep angle and Mach number on the drag at zero lift are shown in figure 9. At Mach numbers below 0.90, the drag coefficient at zero lift coefficient was affected only to a small extent by an increase in sweepback angle and was reduced by an increase in sweepback angle up to 47° at Mach numbers above 0.90. The drag-rise Mach number $\left(\text{defined as the value where } \frac{dC_D}{dM} = 0.1\right)$ was delayed to higher values and the rate of drag increase with Mach number was reduced by an increase in sweepback angle due to the effectiveness of sweep in reducing the pressure drag. Increasing the sweepback angle from 10.8° to 47° resulted in an increase in the drag-rise Mach number from 0.92 to 0.97. At a Mach number of 1.10 the zero lift-drag coefficient was reduced approximately 26 percent by a change in sweep angle from 10.8° to 47°.

Although there appear to be no theories available which predict the effect of sweep on the drag at zero lift, it has been found that the maximum pressure-drag coefficient, which usually occurs in the transonic range, decreases by the fourth power of the cosine of the sweep angle when the thickness ratio remains constant in planes normal to the sweep line. Using the methods described in reference 13 calculations have been made to determine the effect of sweep on the maximum pressure drag at transonic speeds. The expression for the maximum pressure drag as given in reference 13 is

$$C_{D'_{max}} = K\left(\frac{t/c}{\cos \Lambda}\right)^{5/3} \cos^4 \Lambda$$

where

$$K = \frac{\partial C_{D'}}{\partial (t/c)^{5/3}}$$

For these calculations the body-alone data of reference 4 have been subtracted from the experimental results at zero lift such that the data of the present wings presented in figures 10 and 11 represent wing-plus-wing-body-interference data. An experimental value of 2.39 for K obtained from figure 10 has been used in the preceding equation. Unfortunately, only one experimental point for the wing of 10.8° sweep was used to determine the value of K for the present investigation. It was shown in reference 13 that the variation of the pressure drag at a Mach number of 1.00 is fairly linear with $(t/c)^{5/3}$ and can be used to estimate the maximum pressure-drag coefficient of sweptback wings. Figure 11 shows a comparison of the results using the preceding equation with the experimental results obtained from figure 9. It will be noted that the agreement between the calculations and the experimental results is good for the wings of the present investigation.

Figure 12 shows the effect of wing sweep on the drag-due-to-lift parameter at a lift coefficient of 0.3 for Mach numbers of 0.50, 0.90, 1.00, and 1.10. Also shown is the drag-due-to-lift parameter for no leading-edge suction $\frac{1}{57.3\ C_{L_\alpha}}$. Full leading-edge suction $\frac{1}{\pi A}$ for the present wings would be represented by a theoretical value of drag due to lift of 0.091. The results indicated that as the Mach number increased from 0.50 to 1.10 the drag due to lift increased and had a tendency to approach the value of drag due to lift for no leading-edge suction. The results also indicated that the drag due to lift was not greatly affected by sweep angle for the various Mach numbers shown. The fact that the 10.8° sweptback wing retained some leading-edge suction at a Mach number of 1.10, even though the linearized supersonic theories predict no leading-edge suction for wings having their leading edges located ahead of the Mach line, is probably due to the fact that, as indicated by schlieren photographs, a detached bow wave existed ahead of the wing and, therefore, a part of the wing was operating at subsonic velocities.

The effect of sweep angle on the variation of maximum lift-drag ratio with Mach number presented in figure 13 indicated that, at Mach numbers below 0.80, the maximum lift-drag ratio was approximately the same for the configurations with sweep angles of 10.8° and 35°, and was approximately 10 to 14 percent higher for the wing of 47° sweepback. This was probably due to the fact that the drag at zero lift for the wing of 47° sweepback was less than for either the 10.8° or 35° sweptback wings. At the higher subsonic Mach numbers large losses in the values of $(L/D)_{max}$ occurred, and these losses were delayed to higher Mach numbers as the sweep angle was increased. The Mach number where large losses in $(L/D)_{max}$ occurred was delayed from 0.80 to 0.92 as the angle of sweepback was increased from 10.8° to 47°. At a Mach number of 1.10, the maximum lift-drag ratio was increased by a factor of 1.3 with an increase in sweepback angle from 10.8° to 47°.

[redacted]

The effect of compressibility on the lift coefficient corresponding to the maximum lift-drag ratio is shown in figure 14. Increasing the sweepback angle not only decreased the value of lift coefficient corresponding to the maximum lift-drag ratio but also reduced the positive shift in lift coefficient for $(L/D)_{max}$ as the Mach number increased from 0.50 to 1.10. The shift in the lift coefficient for $(L/D)_{max}$ for the configuration with 10.8° sweepback was approximately 59 percent as compared with 40 percent for the configuration with 47° sweepback.

Pitching-Moment Characteristics

The variations of pitching-moment coefficient with lift coefficient (figs. 5(c), 6(c), and 7(c)) were generally nonlinear up to a Mach number of 0.975 for all the sweep configurations. It is interesting to note that for sweepback angles of 10.8° and 47° and at the low Mach numbers, the pronounced breaks in the pitching-moment curves changed from stable breaks to unstable breaks whereas no pronounced breaks were indicated for the 35° sweptback wing. As the Mach number increased beyond 0.975 the pitching-moment curves showed linear variations up to the highest lift coefficient investigated for the three sweep configurations.

The effects of Mach number on the static-longitudinal-stability parameter dC_m/dC_L for the three wings are shown for two lift coefficients in figure 15. The data indicate a general rearward movement of the aerodynamic center with increasing Mach number for the three sweep configurations. As the Mach number was increased from 0.50 to 1.10 for zero lift, the aerodynamic center for the 10.8° sweptback wing moved rearward 18 percent as compared with a 15-percent rearward movement of the aerodynamic center for the 35° and 47° sweptback wings. The rearward movement of the aerodynamic center for the 10.8° sweptback wing was probably associated with a rearward movement of strong shocks on the upper surface of the wing as the Mach number increased. On the other hand, the smaller movement of the aerodynamic center noted for the 35° and 47° sweptback wings, even though there were shock formations on these wings, was probably associated with an outboard movement of the flow in the boundary layer (reference 14) which resulted in a separation of the flow at the tips. This flow separation for the configurations with 35° and 47° of sweepback would prevent the aerodynamic center from moving as far rearward as the aerodynamic center for the wing with a sweepback angle of 10.8°.

[redacted]

CONCLUSIONS

An investigation was made in the Langley 8-foot transonic tunnel of the effects of wing sweepback angle on the aerodynamic characteristics of a wing-body configuration. All the wing models had 4-percent-thick sections parallel to the model plane of symmetry, an aspect ratio of 3.5, and a taper ratio of 0.2. Sweepback angles of 10.8°, 35°, and 47° based on the 0.25-chord line were investigated. The following conclusions are indicated:

1. For the wings of the present investigation an increase in sweepback angle from 10.8° to 47° had only a negligible effect on the lift-curve break Mach number at a lift coefficient of zero.

2. The drag-rise Mach number was delayed to higher values and the rate of drag increase after the drag-rise Mach number was reduced by an increase in sweepback angle due to the effectiveness of sweep in reducing the pressure drag. For the wings of the present investigation, the effect of sweep on the maximum pressure-drag coefficient was estimated fairly accurately using an empirical relationship.

3. The Mach number where large losses in the values of maximum lift-drag ratio occurred was delayed from 0.80 to 0.92 as the angle of sweepback was increased from 10.8° to 47°. At a Mach number of 1.10, the maximum lift-drag ratio was increased by a factor of 1.3 for a similar increase in sweep.

4. An increase in sweepback angle reduced the rearward movement of the aerodynamic-center location as the Mach number increased from 0.50 to 1.10.

Langley Aeronautical Laboratory
National Advisory Committee for Aeronautics
Langley Field, Va.

[redacted]

REFERENCES

1. Robinson, Ross B., and Driver, Cornelius: Aerodynamic Characteristics at Supersonic Speeds of a Series of Wing-Body Combinations Having Cambered Wings with an Aspect Ratio of 3.5 and a Taper Ratio of 0.2. Effects of Sweep Angle and Thickness Ratio on the Aerodynamic Characteristics in Pitch at M = 1.60. NACA RM L51K16a, 1952.

2. Spearman, M. Leroy, and Hilton, John H., Jr.: Aerodynamic Characteristics at Supersonic Speeds of a Series of Wing-Body Combinations Having Cambered Wings with an Aspect Ratio of 3.5 and a Taper Ratio of 0.2. Effects of Sweep Angle and Thickness Ratio on the Static Lateral Stability Characteristics at M = 1.60. NACA RM L51K15a, 1952.

3. Hasel, Lowell E., and Sevier, John R., Jr.: Aerodynamic Characteristics at Supersonic Speeds of a Series of Wing-Body Combinations Having Cambered Wings with an Aspect Ratio of 3.5 and a Taper Ratio of 0.2. Effect at M = 1.60 of Nacelle Shape and Position on the Aerodynamic Characteristics in Pitch of Two Wing-Body Combinations with 47° Sweptback Wings. NACA RM L51K14a, 1952.

4. Bielat, Ralph P., Harrison, Daniel E., and Coppolino, Domenic A.: An Investigation at Transonic Speeds of the Effects of Thickness Ratio and of Thickened Root Sections on the Aerodynamic Characteristics of Wings with 47° Sweepback, Aspect Ratio 3.5, and Taper Ratio 0.2 in the Slotted Test Section of the Langley 8-Foot High-Speed Tunnel. NACA RM L51I04a, 1951.

5. Wright, Ray H., and Ritchie, Virgil S.: Characteristics of a Transonic Test Section with Various Slot Shapes in the Langley 8-Foot High-Speed Tunnel. NACA RM L51H10, 1951.

6. Osborne, Robert S.: A Transonic-Wing Investigation in the Langley 8-Foot High-Speed Tunnel at High Subsonic Mach Numbers and at a Mach Number of 1.2. Wing-Fuselage Configuration Having a Wing of 45° Sweepback, Aspect Ratio 4, Taper Ratio 0.6, and NACA 65A006 Airfoil Section. NACA RM L50H08, 1950.

7. Wright, Ray H., and Ward, Vernon G.: NACA Transonic Wind-Tunnel Test Sections. NACA RM L8J06, 1948.

8. DeYoung, John: Theoretical Additional Span Loading Characteristics of Wings with Arbitrary Sweep, Aspect Ratio, and Taper Ratio. NACA TN 1491, 1947.

[redacted]

9. Ritchie, Virgil S., and Pearson, Albin O.: Calibration of the Slotted Test Section of the Langley 8-Foot Transonic Tunnel and Preliminary Experimental Investigation of Boundary-Reflected Disturbances. NACA RM L51K14, 1952.

10. Fisher, Lewis R.: Approximate Corrections for the Effects of Compressibility on the Subsonic Stability Derivatives of Swept Wings. NACA TN 1854, 1949.

11. Piland, Robert O.: Summary of the Theoretical Lift, Damping-in-Roll, and Center-of-Pressure Characteristics at Various Wing Plan Forms of Supersonic Speeds. NACA TN 1977, 1949.

12. Malvestuto, Frank S., Jr., Margolis, Kenneth, and Ribner, Herbert S.: Theoretical Lift and Damping in Roll at Supersonic Speeds of Thin Sweptback Tapered Wings with Streamwise Tips, Subsonic Leading Edges, and Supersonic Trailing Edges. NACA Rep. 970, 1950. (Supersedes NACA TN 1860.)

13. Polhamus, Edward C.: Summary of Results Obtained by Transonic-Bump Method on Effects of Plan Form and Thickness on Lift and Drag Characteristics of Wings at Transonic Speeds. NACA RM L51H30, 1951.

14. Whitcomb, Richard T.: An Experimental Study at Moderate and High Subsonic Speeds of the Flow over Wings with 30° and 45° of Sweepback in Conjunction with a Fuselage. NACA RM L50K27, 1951.

[redacted]

TABLE I.- AIRFOIL COORDINATES

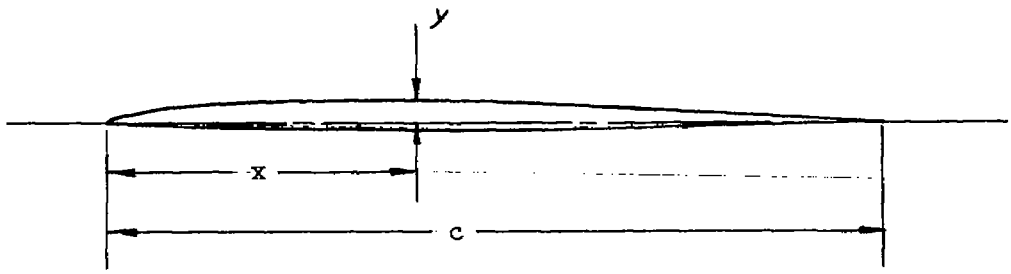

x/c (percent)	y/c upper surface (percent)	y/c lower surface (percent)
0	0	0
.5	.411	.245
.75	.499	.271
1.25	.665	.289
2.5	.962	.324
5.0	1.435	.367
7.5	1.776	.429
10.0	2.039	.472
15	2.423	.577
20	2.642	.682
25	2.800	.787
30	2.887	.892
35	2.983	.997
40	2.992	1.006
45	2.940	1.041
50	2.852	1.006
55	2.712	.945
60	2.511	.857
65	2.265	.761
70	1.986	.674
75	1.680	.577
80	1.356	.481
85	1.041	.385
90	.726	.289
95	.402	.201
100	.105	.105
L.E. radius = 0.0016c		

[redacted]

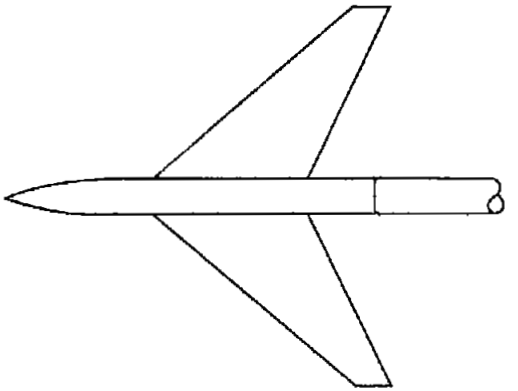

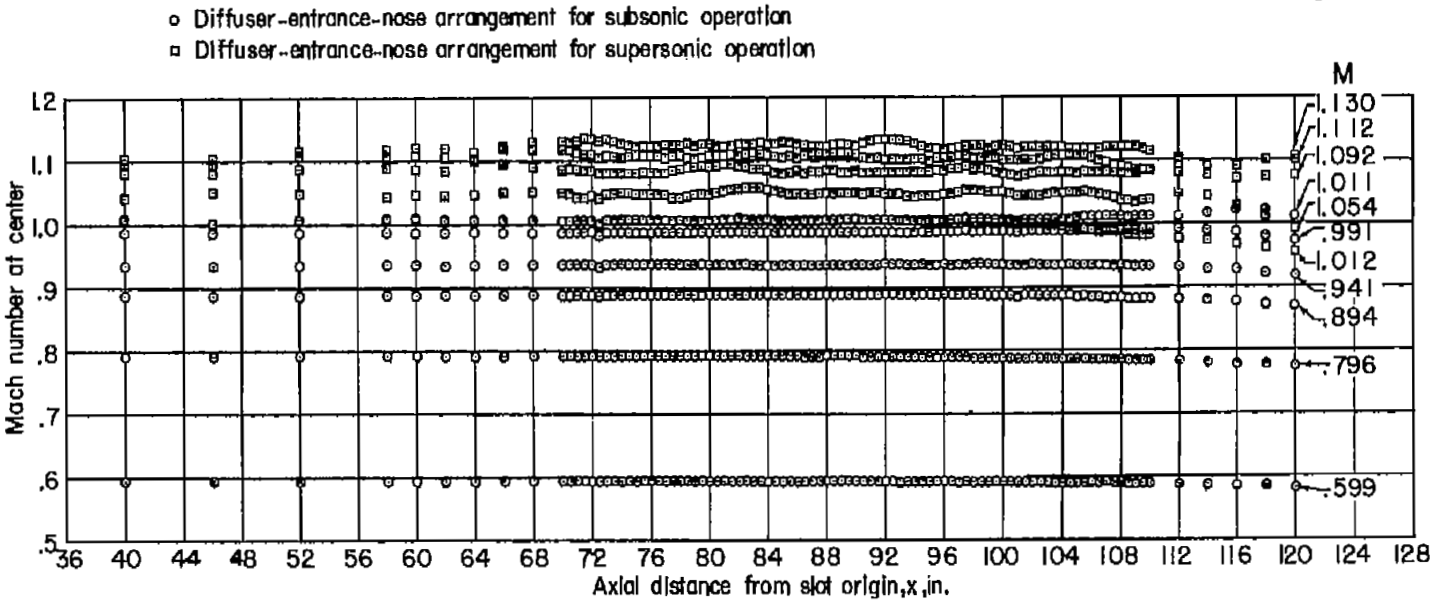

Figure 1.- Mach number distributions along the center of the test section.

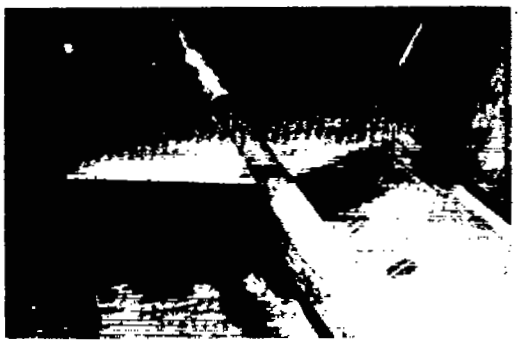

$\Lambda = 10.8^{\circ}$ NACA L-71808

$\Lambda = 35^{\circ}$ NACA L-71807

$\Lambda = 47^{\circ}$ NACA L-71309.1

Figure 2.- Photographs of models as tested in the Langley 8-foot transonic tunnel.

Airfoil section parallel to plane of symmetry	
Thickness distribution	NACA 65A series
Mean line ordinates	1/3 of NACA 230 series + NACA 6-series uniform-load mean line (a = 1.0) for $C_{l_1} = 0.1$
Area, sq ft	1.143
Aspect ratio	3.5
Taper ratio	0.2
Incidence, deg	0
Dihedral, deg	0
Geometric twist, deg	0

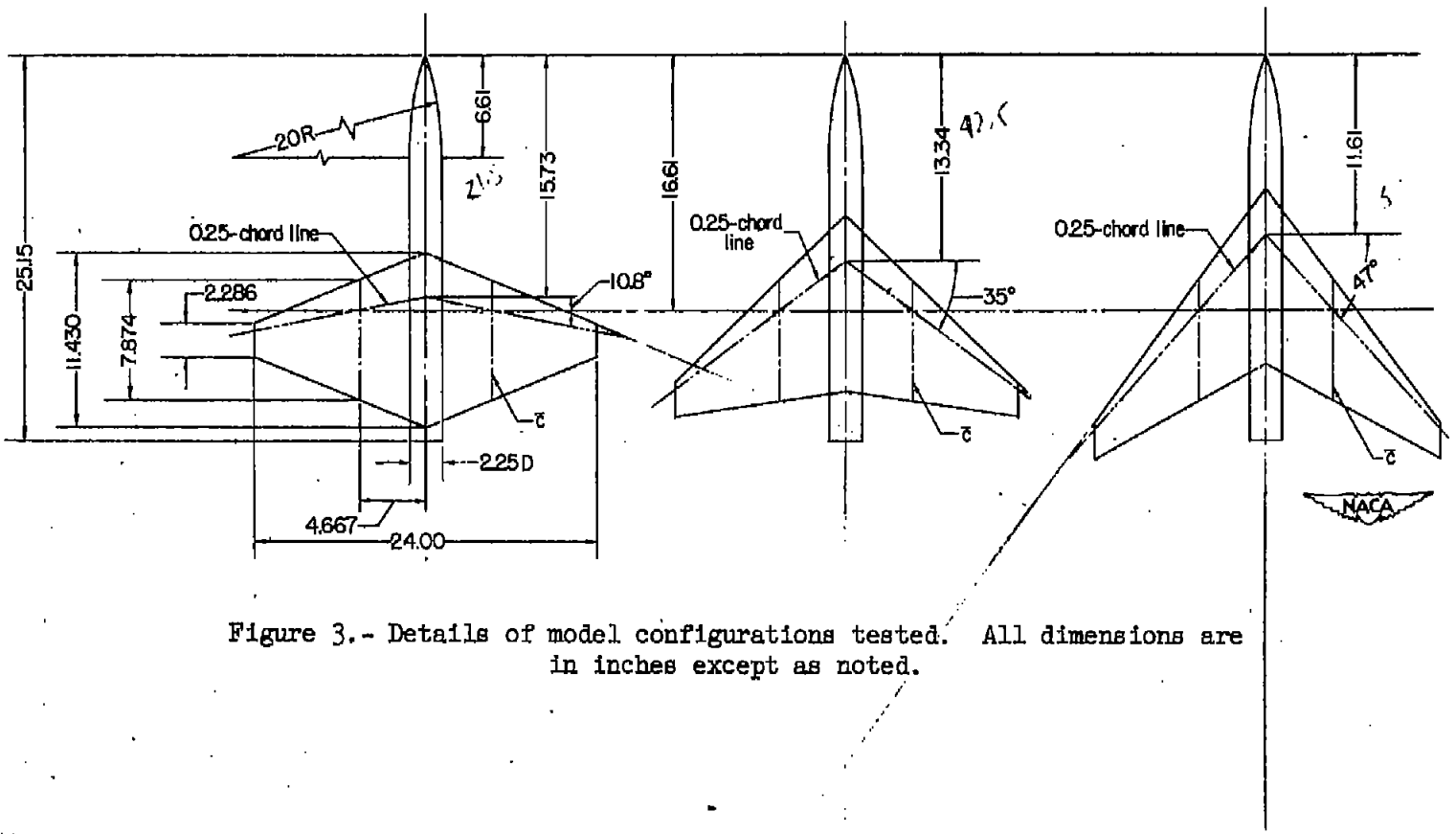

Figure 3.- Details of model configurations tested. All dimensions are in inches except as noted.

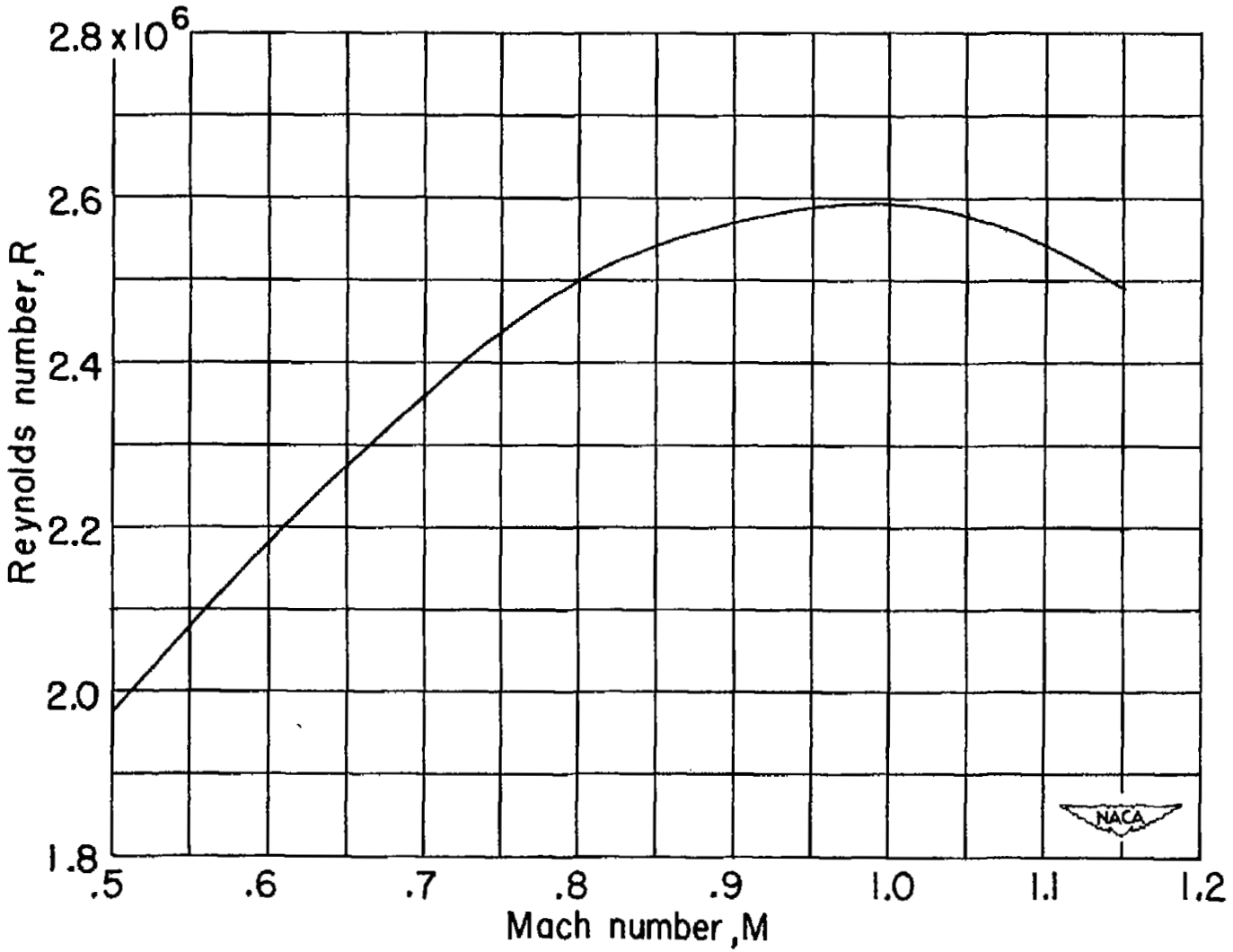

Figure 4.- Variation with Mach number of test Reynolds number based on a mean aerodynamic chord of 7.874 inches.

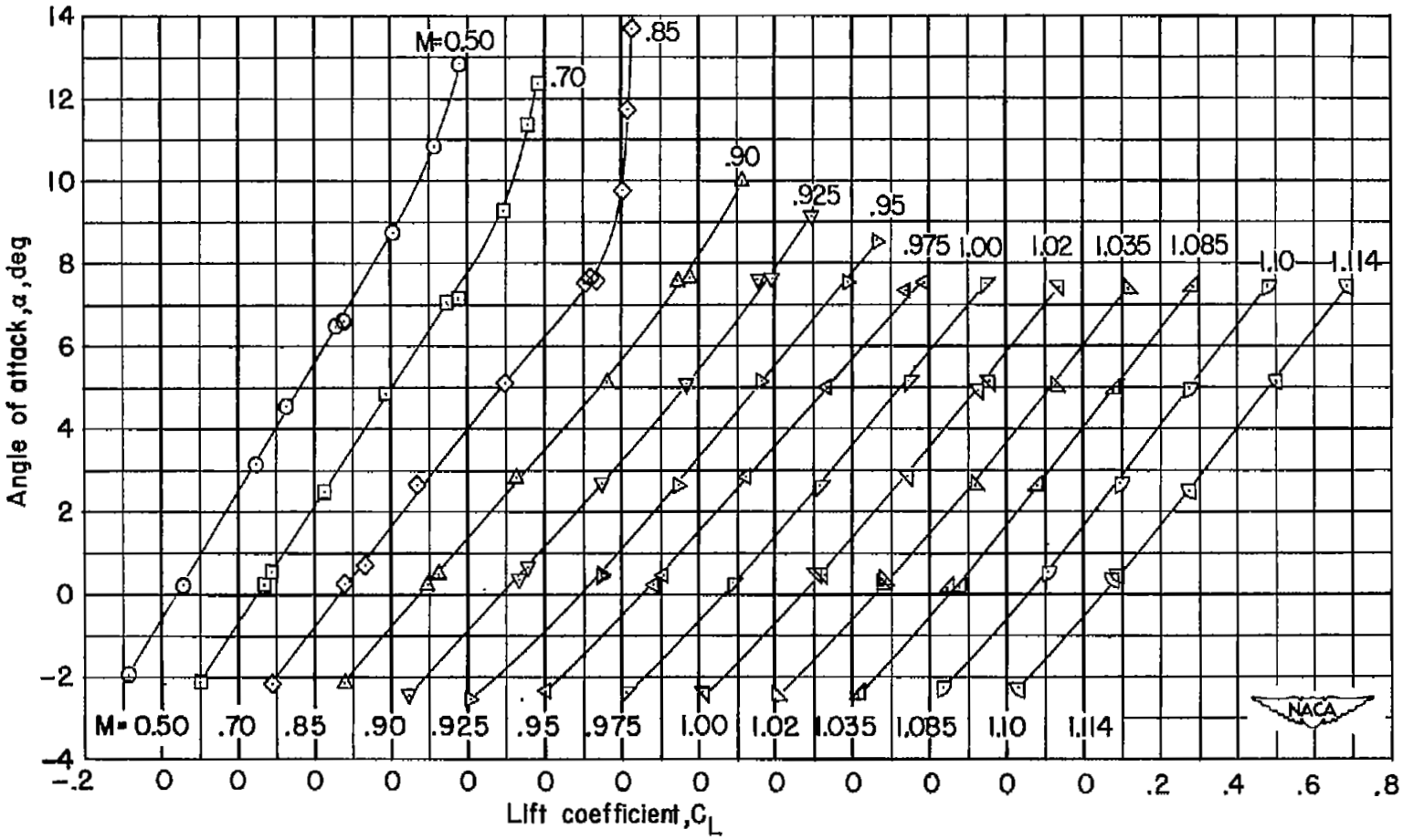

(a) Angle of attack.

Figure 5.- Variation with lift coefficient of the aerodynamic characteristics for the 10.8° sweptback wing.

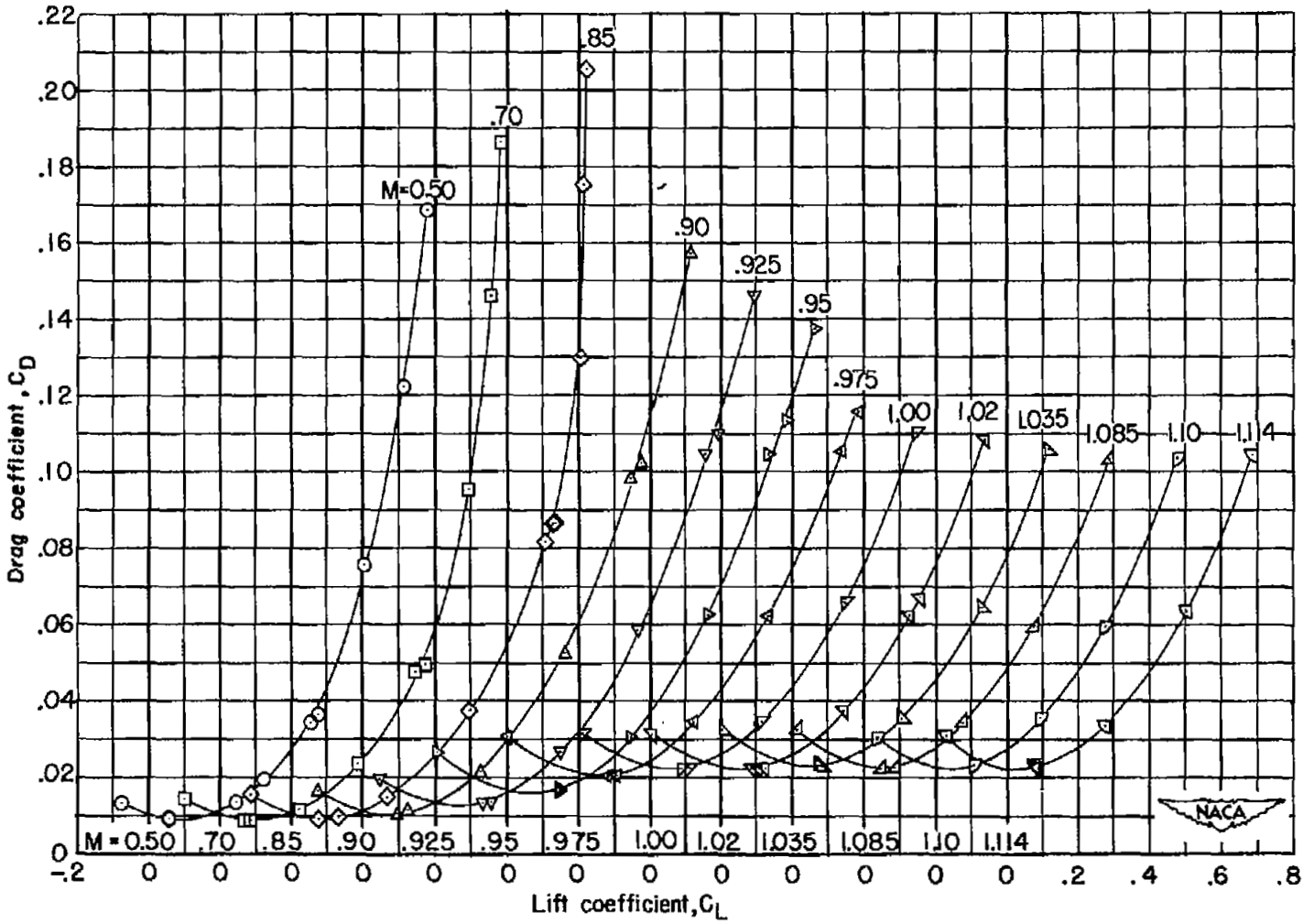

(b) Drag coefficient.

Figure 5.- Continued.

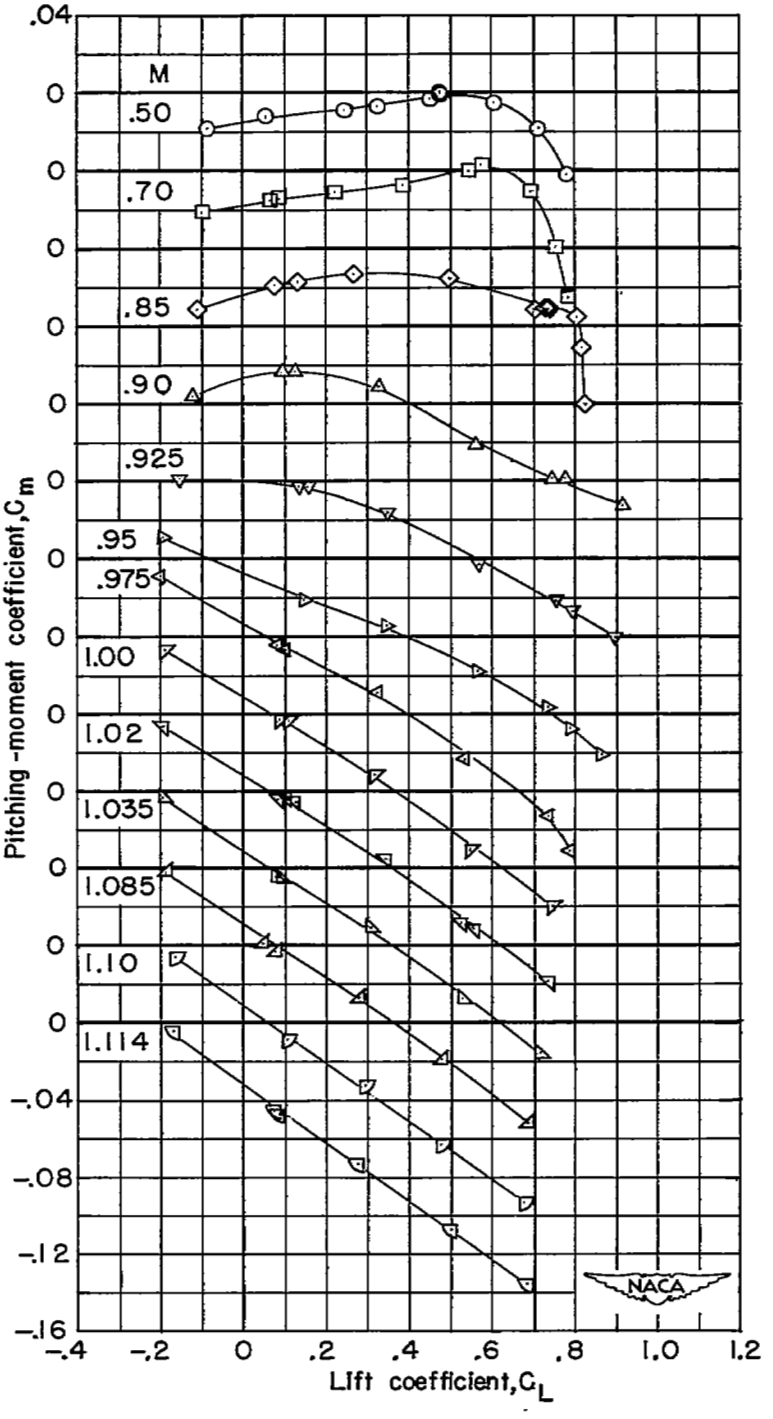

(c) Pitching-moment coefficient.

Figure 5.- Concluded.

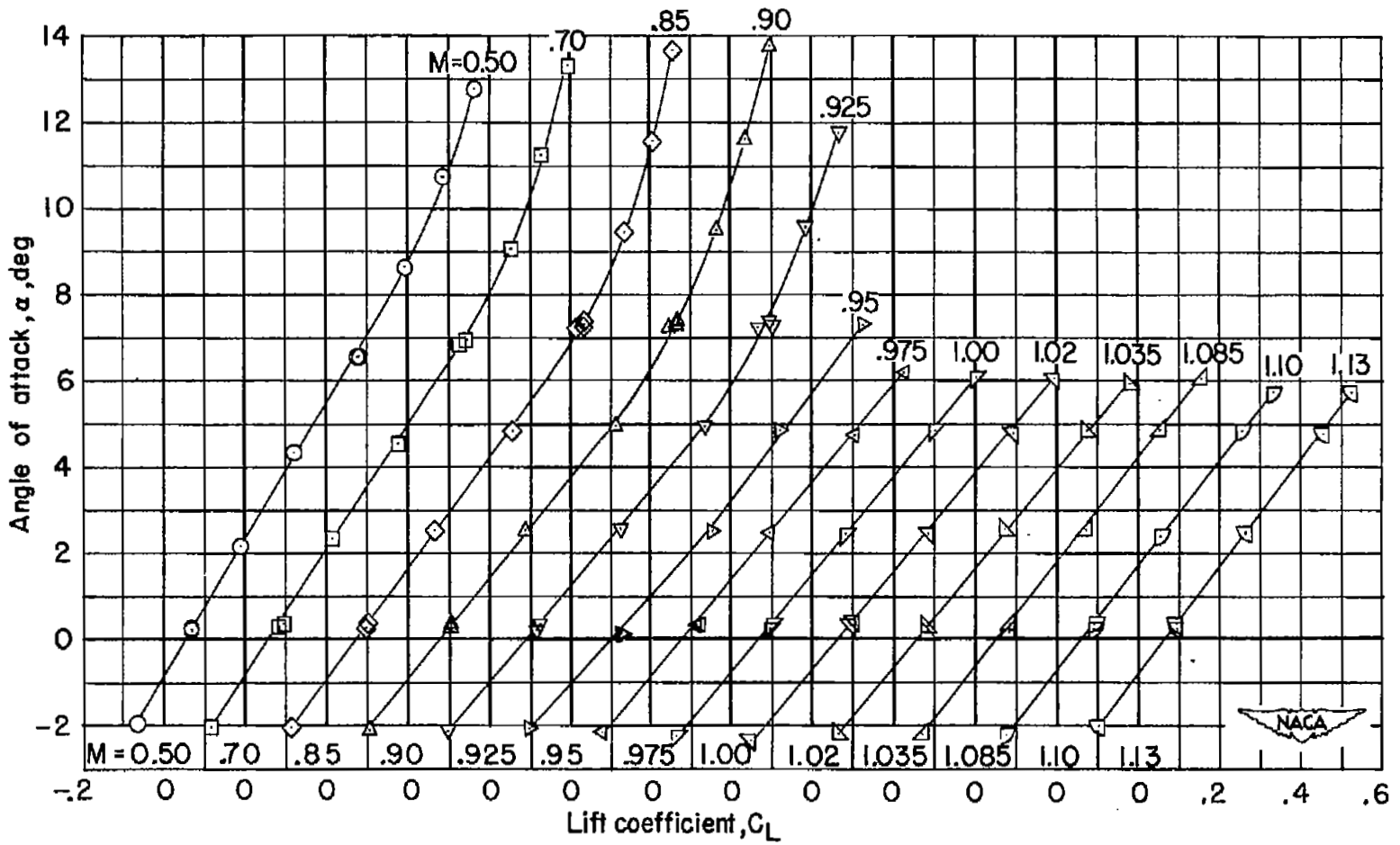

(a) Angle of attack.

Figure 6.- Variation with lift coefficient of the aerodynamic characteristics for the 35° sweptback wing.

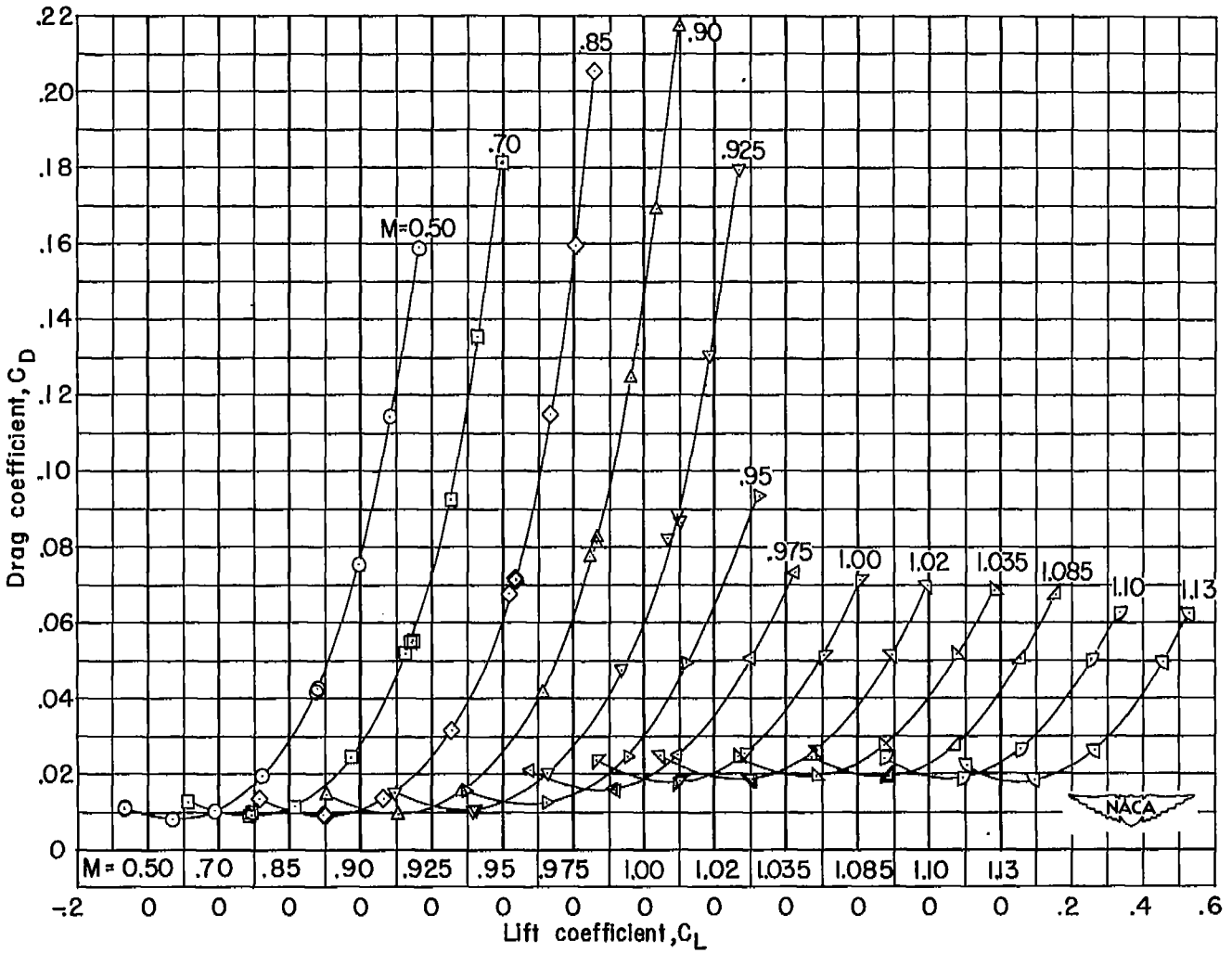

(b) Drag coefficient.

Figure 6.- Continued.

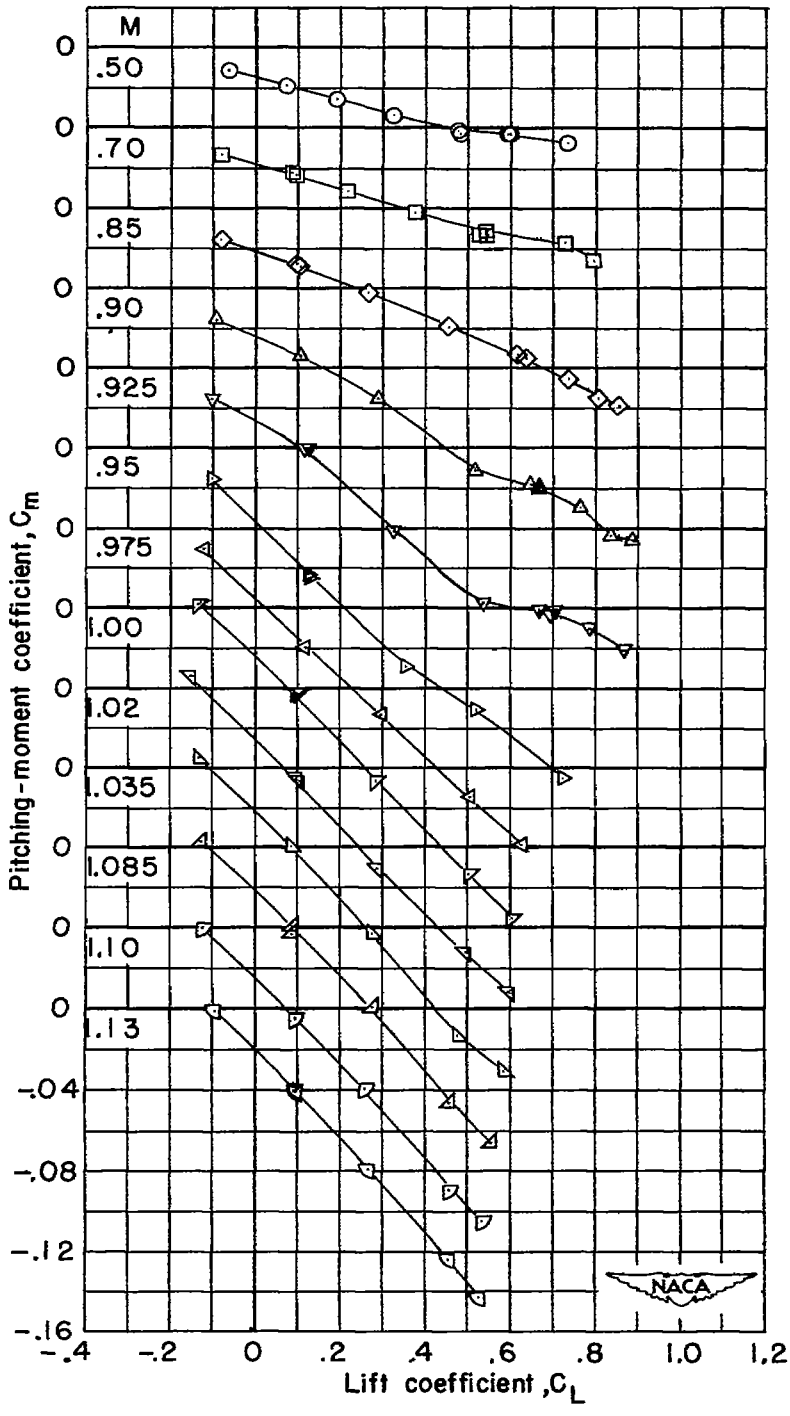

(c) Pitching-moment coefficient.

Figure 6.- Concluded.

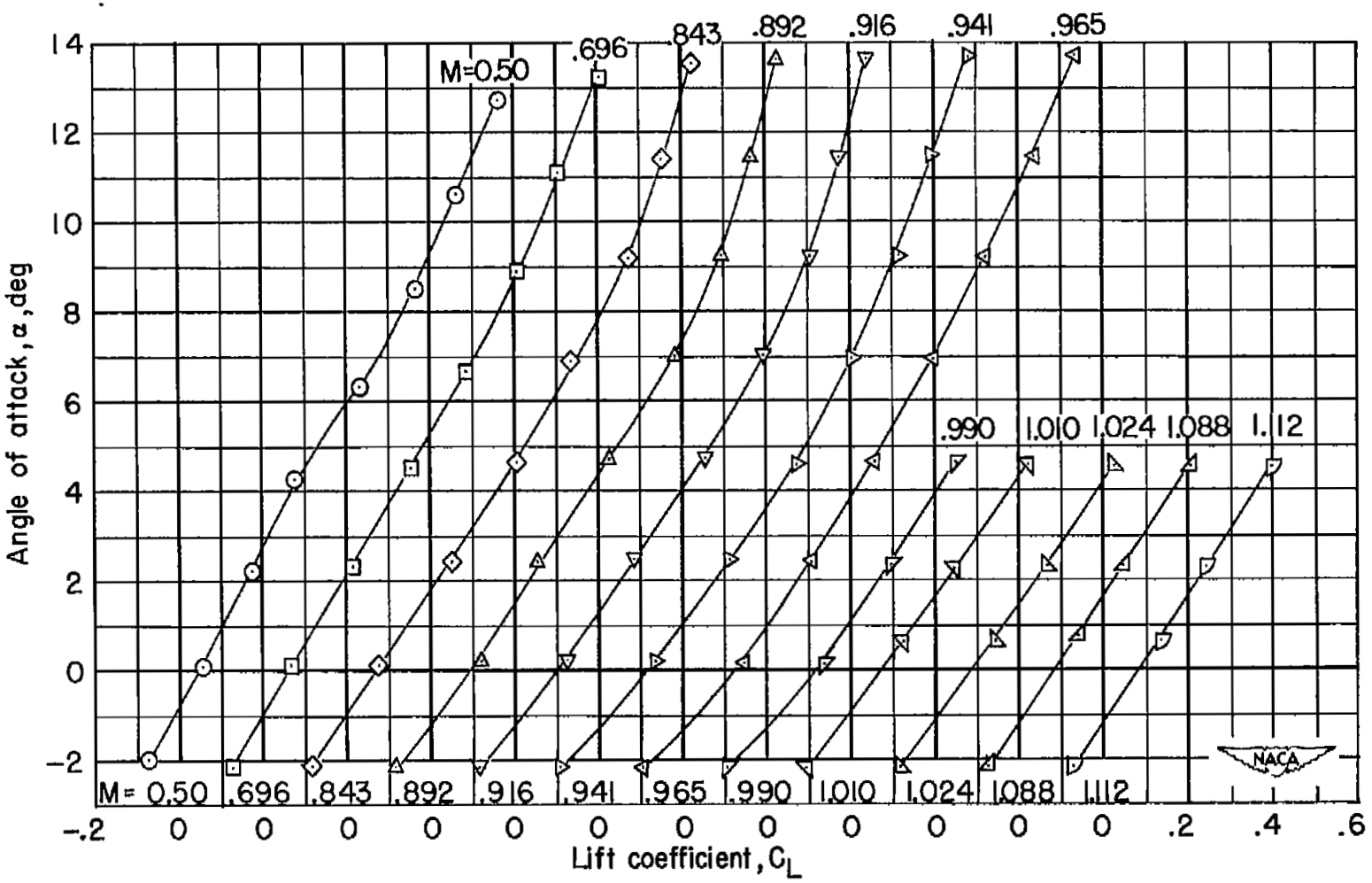

(a) Angle of attack.

Figure 7.- Variation with lift coefficient of the aerodynamic characteristics for the 47° sweptback wing.

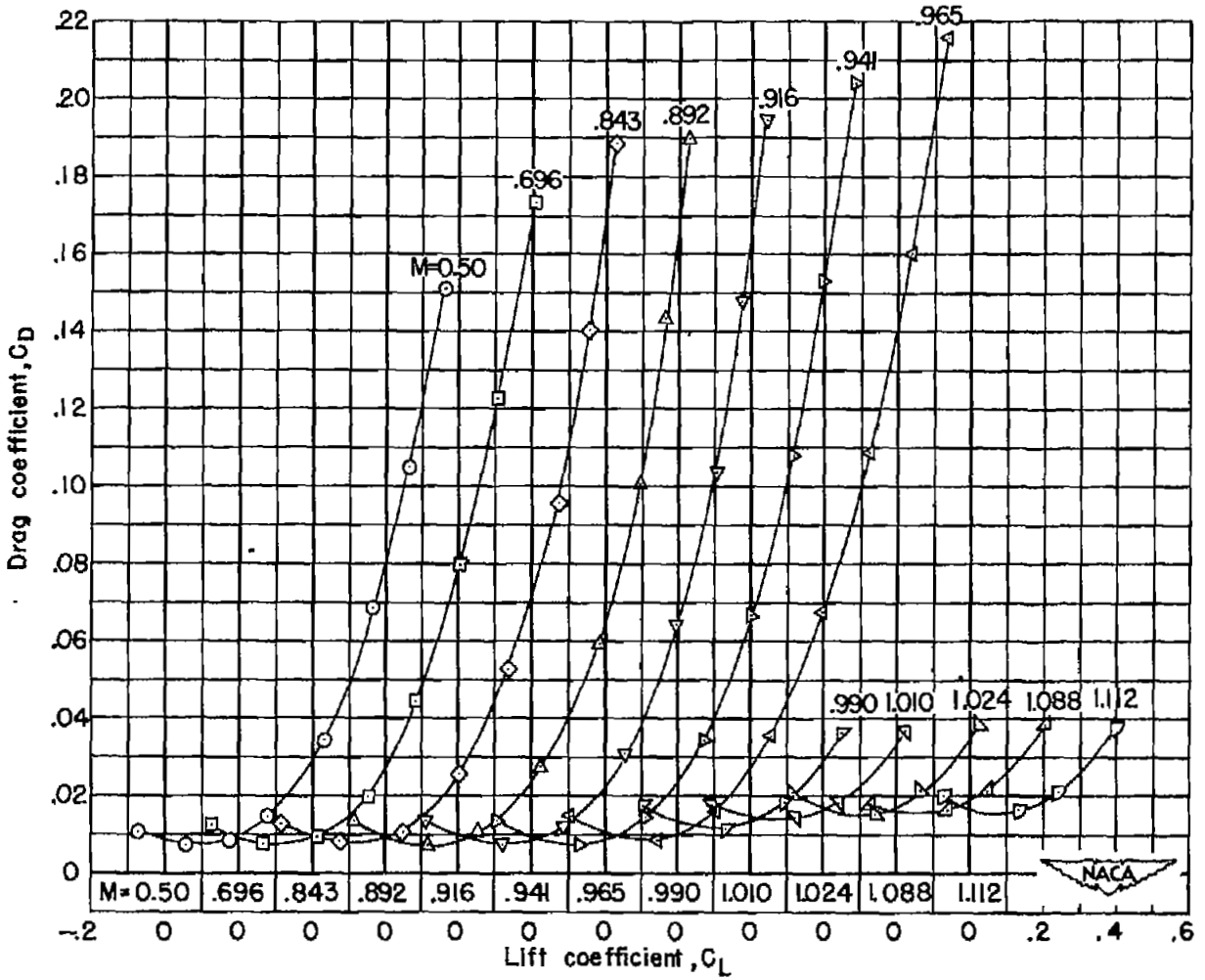

(b) Drag coefficient.

Figure 7.- Continued.

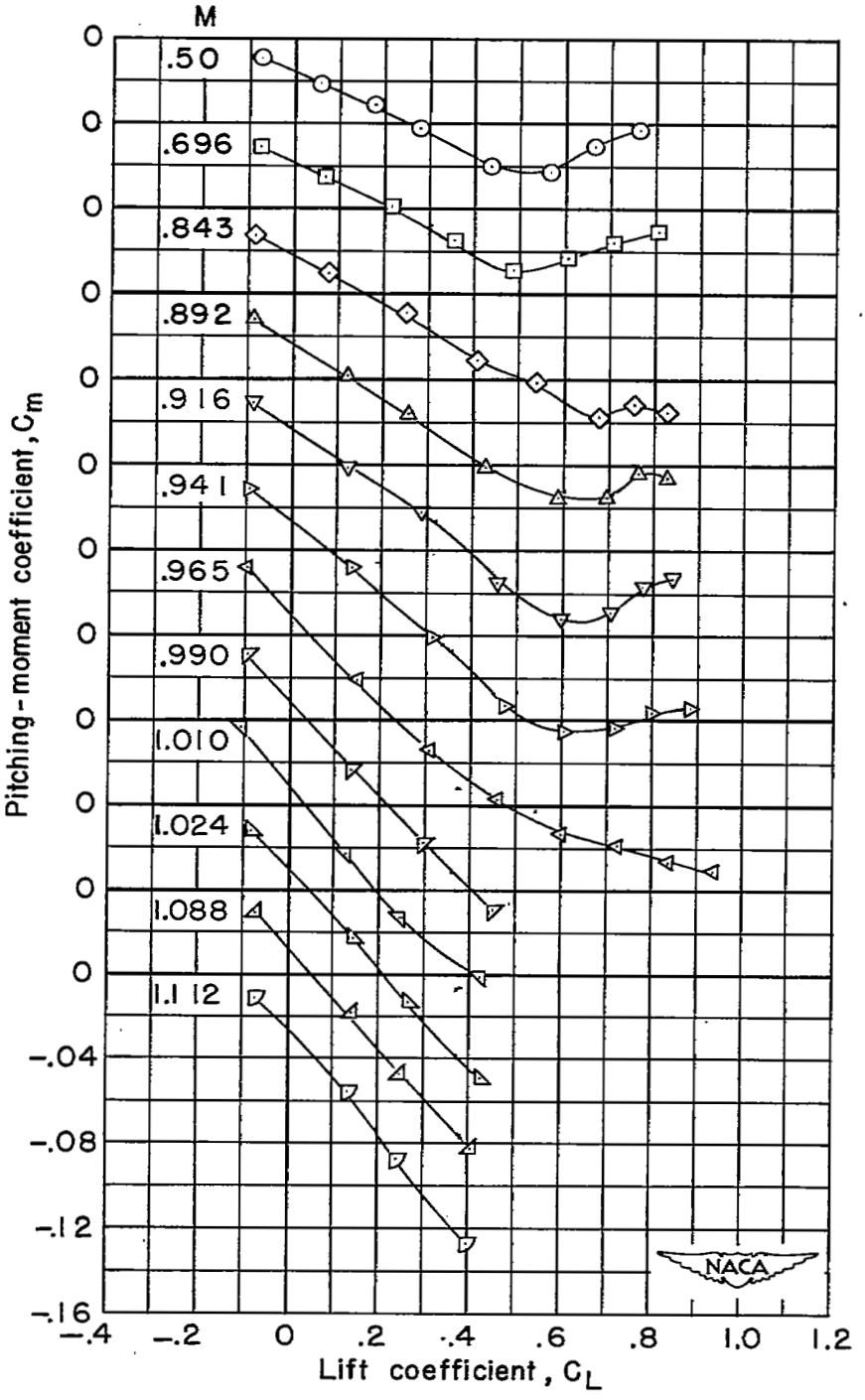

(c) Pitching-moment coefficient.

Figure 7.- Concluded.

[redacted]

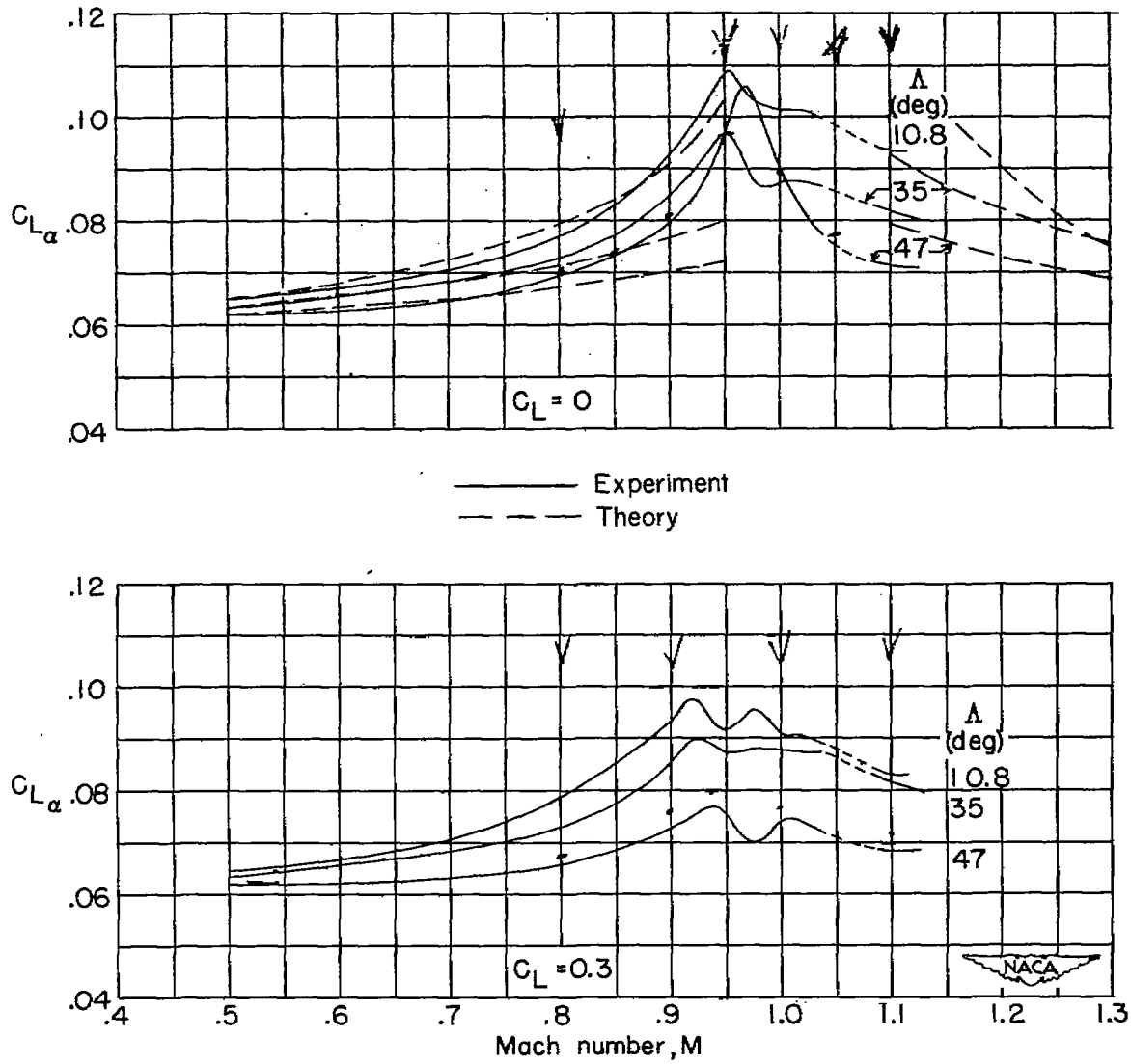

Figure 8.- Effect of sweep angle on the variation of lift-curve slope with Mach number for the wing-body configuration.

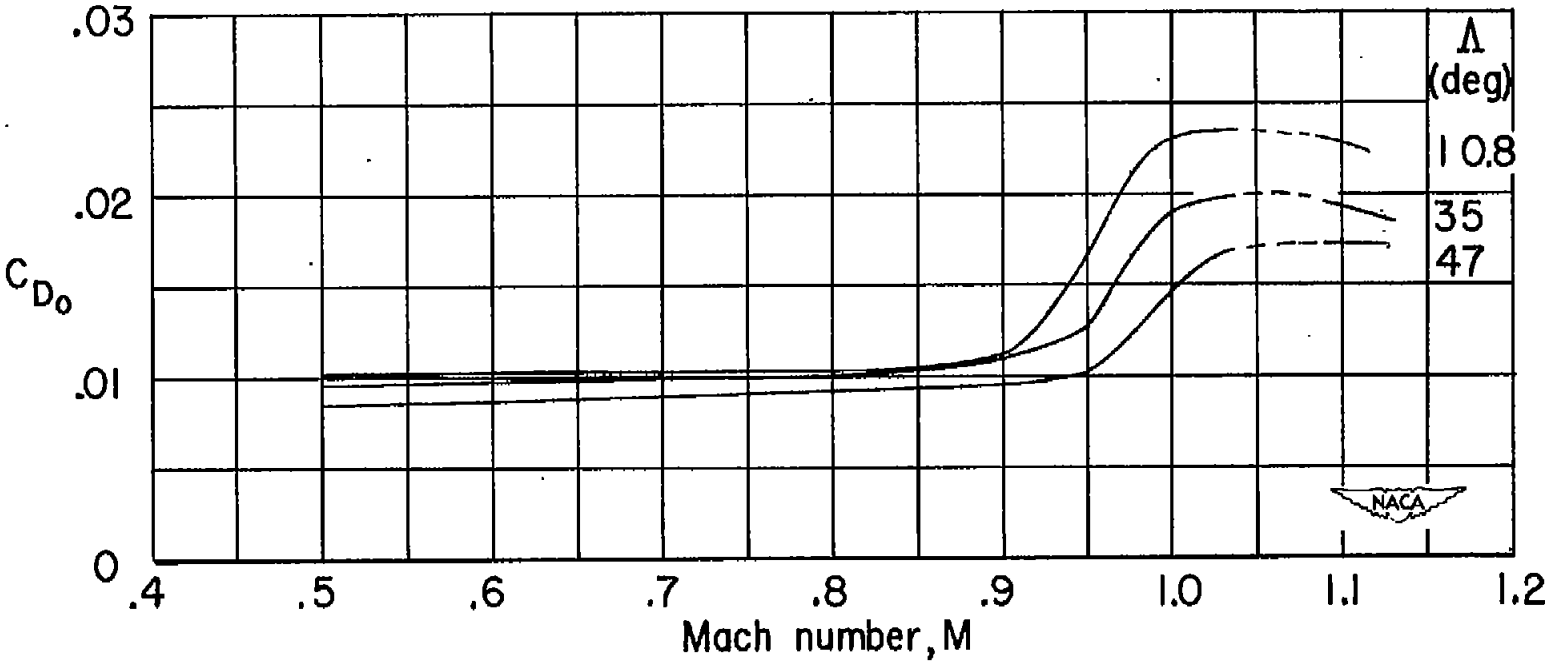

Figure 9.- Effect of sweep angle on the variation of drag coefficient at zero lift with Mach number for the wing-body configuration.

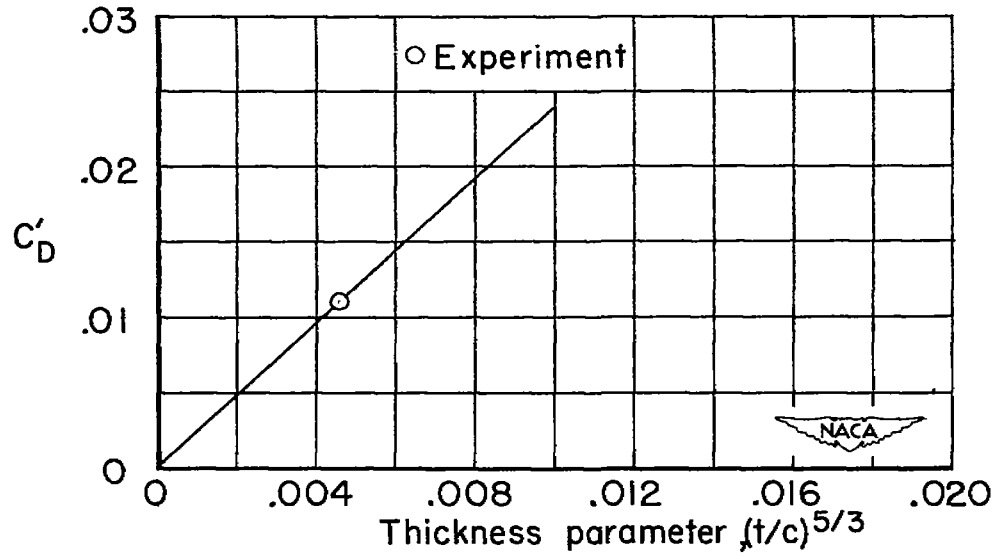

Figure 10.- Effect of thickness ratio on the sonic pressure drag for the wing with wing-body interference.

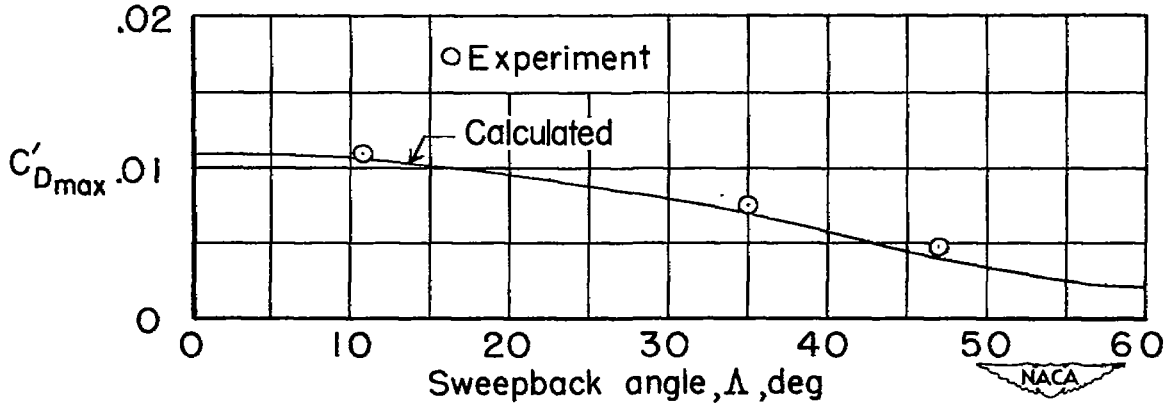

Figure 11.- Effect of sweep angle on the maximum pressure drag at zero lift for the wing with wing-body interference.

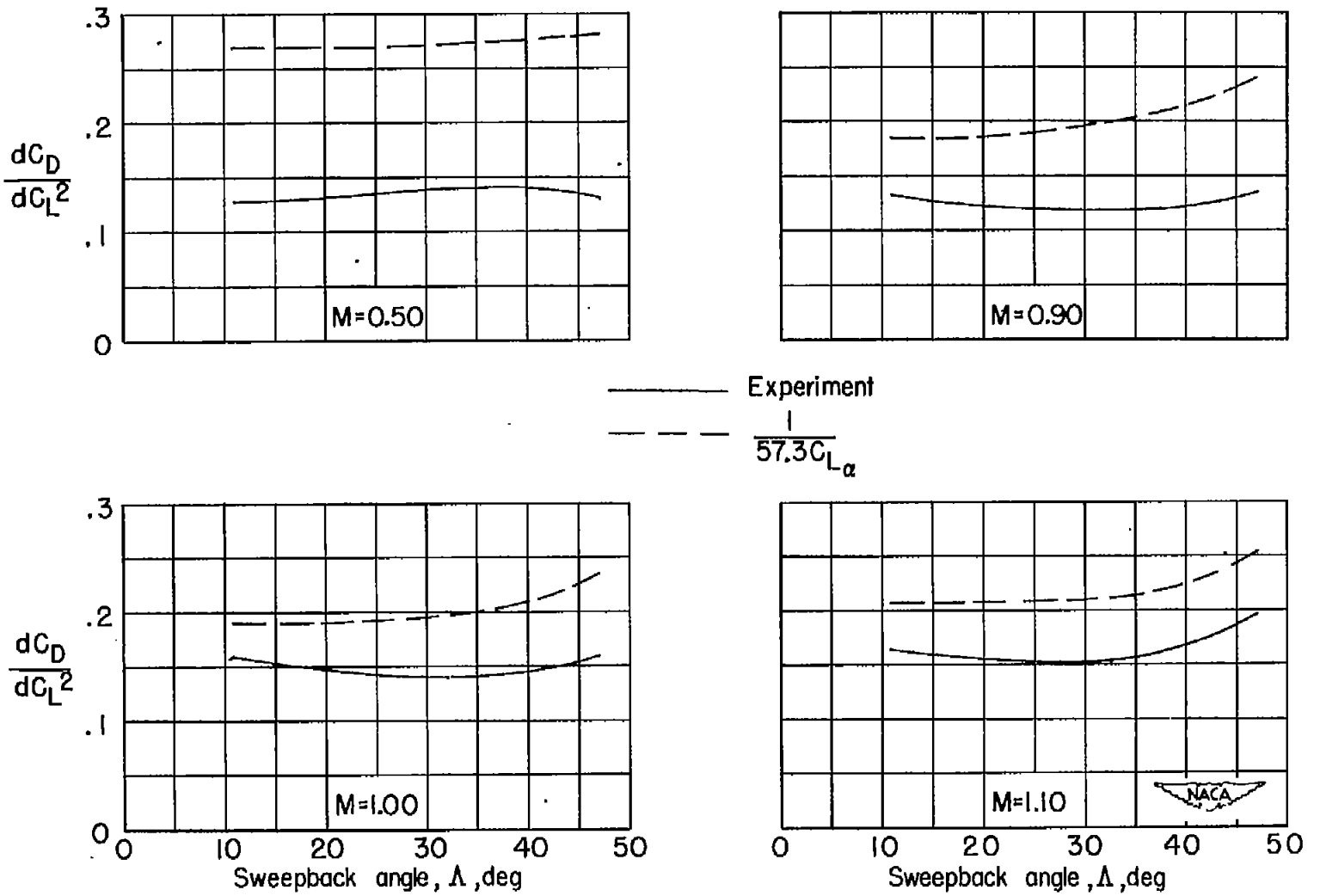

Figure 12.- Effect of sweep angle on the drag due to lift for the wing-body configuration. $C_L = 0.3$.

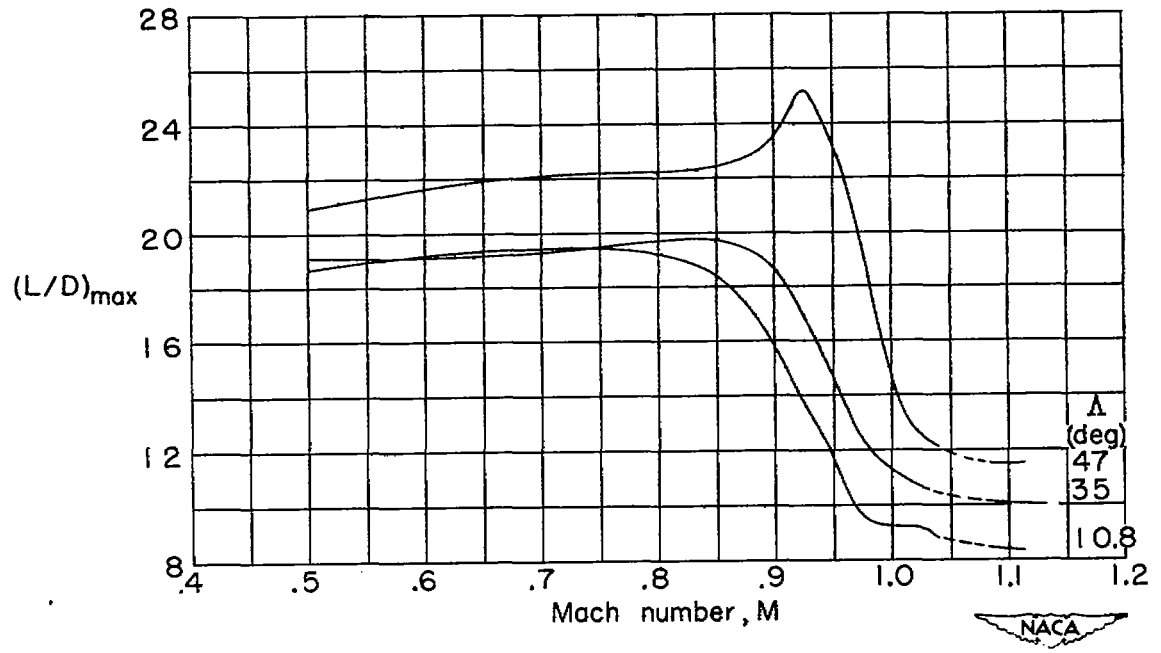

Figure 13.- Effect of sweep angle on the variation of maximum lift-drag ratio with Mach number for the wing-body configuration.

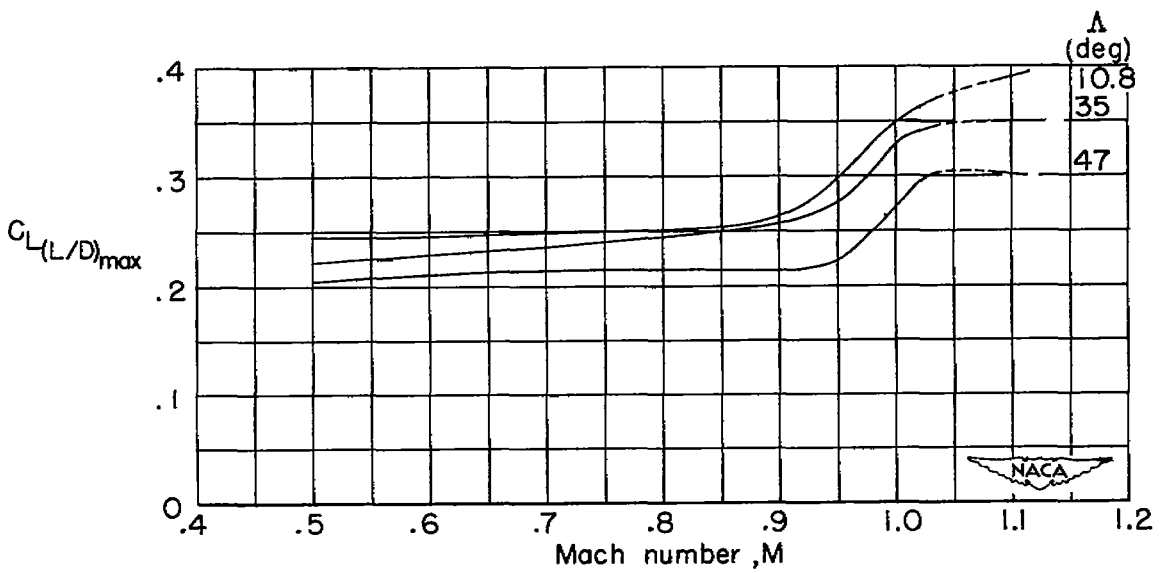

Figure 14.- Effect of sweep angle on the variation of lift coefficient for maximum lift-drag ratio with Mach number for the wing-body configuration.

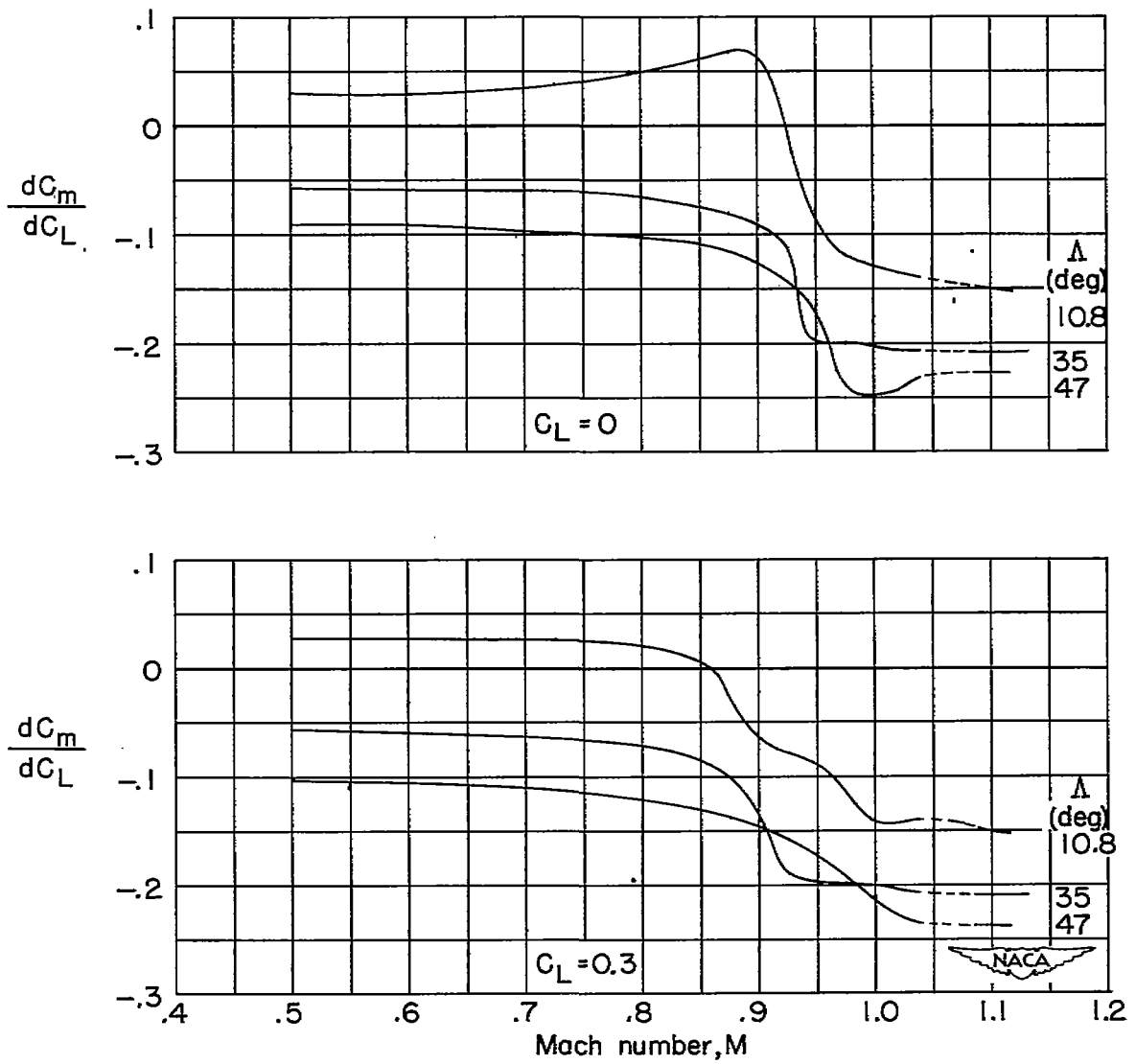

Figure 15.- Effect of sweep angle on the variation of the static-longitudinal-stability parameter with Mach number for the wing-body configuration.

[redacted]

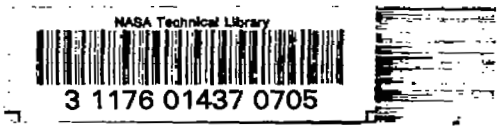

[redacted]